



# DIFFRACTION MODELING FOR SCATTERING OBJECTS WITH NON-RIGID SURFACES

U. Peter Svensson<sup>1\*</sup>

Viggo Henriksen<sup>2</sup>

Herold Olsen<sup>2</sup>

<sup>1</sup> Department of Electronic Systems, NTNU, Trondheim, Norway

<sup>2</sup> SINTEF Digital, Trondheim, Norway

## ABSTRACT

Scattering from rigid, convex objects can be computed accurately and efficiently using the Edge Source Integral Equation. Here, we study the scattering from a rigid object where a part of the surface has an impedance boundary condition (BC). Secondary sources, in the form of virtual pistons, are introduced at the impedance part of the surface. The vibration velocities of the pistons are derived such that they, together with the primary sound field for a rigid BC, fulfill the impedance BC. To derive the virtual piston vibration velocities, the load on the front side of the piston is computed with the rigid BC, and for the rear side a locally reacting impedance BC is specified. Results with this approach are compared with finite-element calculations for a 2D geometry (a 3m by 0.2m box with a 0.3m strip of locally reacting impedance surface) and excellent agreement is found across a frequency range from 50 Hz to 2.5 kHz. Known numerical challenges for the ESIE method are observed for certain scattering directions.

**Keywords:** *scattering, diffraction, secondary sources, impedance boundary condition*

## 1. INTRODUCTION

The scattering of sound by objects generally has to be computed numerically since there are very few shapes which have analytical solutions. Popular numerical methods include the surface-oriented boundary element

*\*Corresponding author: peter.svensson@ntnu.no.*

**Copyright:** ©2023 U. Peter Svensson et al. This is an open-access article distributed under the terms of the Creative Commons Attribution 3.0 Unported License, which permits unrestricted use, distribution, and reproduction in any medium, provided the original author and source are credited.

method (BEM) and volume-oriented methods such as the finite element method (FEM) and finite differences. All of these numerical methods can handle scattering objects with arbitrary shapes and surface impedances. Common for these numerical methods is that the computational cost grows fast with frequency, which might limit their usefulness for larger domains/higher frequencies.

For a special set of scattering objects - convex-shaped objects with rigid surfaces, the so-called edge-source integral equation (ESIE) has been shown to give very accurate results compared to analytical solutions [1] and results computed with the BEM [2]. The edge-source integral equation can not handle non-rigid surfaces directly, so the aim of this paper is to present a method to handle small impedance patches in otherwise rigid objects, based on the ESIE formulation. The approach is to introduce secondary surface sources in the form of virtual pistons, at the locations of impedance surfaces. This secondary-source approach, using solutions for all-rigid boundary conditions, can be found in many studies under various names, such as the blocked impedance method, Thevenin equivalents, or the surface-impedance approach, [3].

## 2. THEORY

### 2.1 The ESIE diffraction model for objects with rigid surfaces

For a scattering problem with a primary sound source and a rigid, convex scattering object, the ESIE diffraction model decomposes the sound field into a sum of geometrical acoustics (GA) and diffraction components. A monopole primary source is located at a source position  $\mathbf{x}_S$ , a receiver at  $\mathbf{x}$ , and furthermore a time-harmonic factor  $e^{j\omega t}$  is assumed but omitted. Then we can introduce transfer functions,  $H$ , for the various components, where

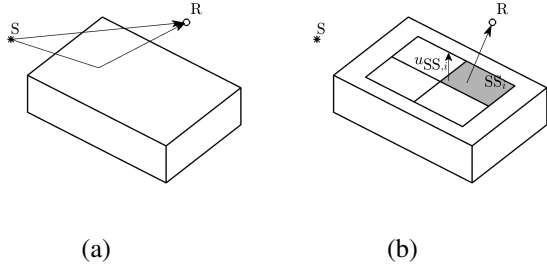


**Figure 1:** The secondary source approach in Eqn. (2) adds (a) the sound field generated by the primary source  $S$  and the rigid scattering object, and (b) the sound fields radiated by secondary piston sources  $SS_i$  with vibration velocities  $u_{SS,i}$ , when pistons are set in a rigid scattering object. Only the GA components are illustrated; diffraction components should be added to both (a) and (b).

we also leave out the notation  $H(\mathbf{x} \leftarrow \mathbf{x}_S)$ ,

$$p_{\text{total}}(\mathbf{x}) = Q_S (H_{\text{direct}} + H_{\text{spec.}} + H_{\text{diff. 1}} + H_{\text{HOD}}) \quad (1)$$

where  $Q_S = j\omega\rho_0 U_0 / (4\pi)$  is the source signal amplitude with  $\rho_0$  being the density of the fluid or gas, and  $U_0$  is the volume velocity of the monopole source. The details are described in [1] and will not be presented here. Briefly, the two first terms,  $H_{\text{direct}}$  and  $H_{\text{spec.}}$ , represent the direct sound and specular reflection, and they involve visibility tests such that the direct sound is zero for receiver positions that are hidden from the source etc. The third term,  $H_{\text{diff. 1}}$ , represents first-order diffraction which is generated by every edge which can be seen by the source and the receiver.  $H_{\text{diff. 1}}$  is computed as an integral over each visible finite edge, [1]. Finally, the fourth term,  $H_{\text{HOD}}$ , contains all second- and higher-order, computed via directional edge source amplitudes which result from solving an integral equation. The edge source amplitudes are then propagated to receiver positions [1].

## 2.2 The secondary source approach, ESIE+SS

If the scattering object has some part of the surface with a non-rigid boundary condition, secondary sources can be introduced to represent such an "impedance patch". A numerically simple approach is to introduce  $N_{SS}$  virtual pistons centered at locations  $\mathbf{x}_{SS,i}$ , and then let these secondary source pistons get a vibration amplitude  $u_{SS,i}$  which, together with the field from the primary sound

source (for a rigid scattering object), generates a field which fulfills the boundary condition at the impedance patch. Once the vibration velocities of the secondary source pistons have been determined, the sound radiated from these pistons can be computed with the ESIE method, for the boundary condition of a rigid scattering body. This can be illustrated as in 1 and formulated as

$$p_{\text{total}}(\mathbf{x}) = Q_S \cdot H + \sum_{i=1}^{N_{SS}} u_{SS,i} \cdot G \quad (2)$$

where the  $G$  transfer functions give the sound pressure for a piston source, with the vibration velocity  $u_{SS}$  being the source signal instead of the  $Q_S$  used for the point-to-point  $H$  transfer functions. The same decomposition as in Eqn. (1) can be used for all the  $G$  transfer functions. The piston velocities,  $u_{SS,i}$ , are found by storing the  $N_{SS}$  unknown, to be determined, values in a vertical array,  $\mathbf{u}_{SS}$ , and formulating a matrix equation,

$$[\mathbf{G}_{\text{front}} + \mathbf{G}_{\text{rear}}] \mathbf{u}_{SS} = \mathbf{p}_{\text{excitation}} \quad (3)$$

where  $\mathbf{p}_{\text{excitation}}$  is a vertical array of the sound pressure amplitudes caused by the primary source at the secondary source pistons' central points with a rigid boundary condition at the piston locations,

$$\mathbf{p}_{\text{excitation}} = [p_{\text{excitation}}(\mathbf{x}_{SS,i})] = Q_S [H(\mathbf{x}_{SS,i} \leftarrow \mathbf{x}_S)]$$

The values in  $\mathbf{u}_{SS}$  can then be found via a matrix inversion based on Eqn. (3), where it is assumed that this inversion exists and can be computed. In Eqn. (3),  $\mathbf{G}_{\text{front}}$  is a square matrix of interaction transfer functions between all the  $N_{SS}$  secondary source pistons,  $G_{\text{front},ij} = G_{\text{front, SS mid-point } i \leftarrow \text{SS piston } j}$ . The second matrix in Eqn. (3),  $\mathbf{G}_{\text{rear}}$ , describes the transfer functions into the impedance surface. For a locally reacting impedance material model, there is no cross-coupling between the secondary source pistons on the rear side, so  $\mathbf{G}_{\text{rear}} = Z_{s,\text{target}} \mathbf{I}$ , where  $\mathbf{I}$  is the identity matrix of size  $(N_{SS}, N_{SS})$  and  $Z_{s,\text{target}}$  is the target (specific acoustic) impedance value at the impedance material.

## 3. NUMERICAL EXAMPLE

To evaluate the "ESIE+SS" approach, a rigid box with a small impedance patch was modeled in 2D. The scattering was computed using the FEM, as implemented in the COMSOL software [4], as a reference result, and with the ESIE+SS method. Fig. 2 shows the ESIE model as well

as the FEM geometry, with a circle of receivers around the box. The impedance patch was given a locally reacting impedance boundary condition, with values representing a 200 mm thick porous material against a rigid wall. The flow resistivity was  $10 \text{ kPa s/m}^2$  and Mechel's model was used for the modeling, as implemented in the Norflag software [5].

For the FEM modeling, COMSOL Multiphysics, v 6.1, with the Acoustics module was used. The "pressure acoustics" domain indicated in Fig. 2(b) was meshed with triangular elements with a maximum element side length of 6.88 mm. The perfectly matched layer, PML, had a thickness of 5 elements in the radial direction. The ESIE+SS method used the Matlab EDtoolbox available at [6], extended with extra Matlab scripts that implemented the SS approach. In order to model a 2D case with the ESIE method, a 3D model of length  $L$  (in the third dimension) had to be constructed, and some additional steps had to be taken. For the point-to-point  $H$  transfer functions, the direct sound and specular reflection used the free-field expression for a line-source in 3D,  $H = H_0(kr)$ , where  $H_0$  is the Hankel function of zero-th order, replacing the point-source GA components in the EDtoolbox (after proper re-scaling). The first-order diffraction transfer functions were computed with the modal sum approach in [7] while the higher-order diffraction transfer functions were computed by representing the line source by a set of 501 monopoles distributed along the length  $L/2$  (half the length due to symmetry). For the piston-to-point  $G$  transfer functions, the GA components were computed via impulse responses for strip pistons using the method in [8] that were converted to transfer functions via the FFT. The first- and higher-order diffraction components all used a set of 501 monopoles at the center of each strip piston. Table 1 gives the lengths that were used for different frequencies, as well as number of Gaussian quadrature points (edge points) for the higher-order diffraction computations, which used up to 6th order.

#### 4. RESULTS

The sound pressure was computed for the third-octave band frequencies from 50 Hz to 2.5 kHz, the results for two of which are shown in Fig. 3. The receiver ranges marked with grey are those where the computation of higher-order diffraction converges (by increasing the quadrature order) very slowly, as also indicated in Fig. 2 (a). As shown in [2], the so-called ESIEBEM approach could be used to overcome these challenges but it

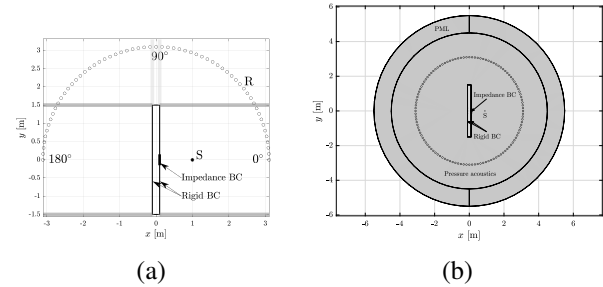


**Figure 2:** Geometrical details for the numerical example with a mostly rigid box, sized 3 m by 0.2 m, and a small patch with a locally reacting impedance boundary condition. A 2D point source is marked S and a half/full circle of receivers is shown as well. In (a), the model for the ESIE+SS approach is shown, and the numerically most challenging receiver directions, for the higher-order diffraction, are marked with darker grey areas, and the more benign challenging directions are marked with lighter grey areas. In (b), the FEM geometry is shown, indicating an outer circle of a perfectly matched layer (PML).

was not implemented here. Since these known challenging positions cause very large errors, median and quantiles for the errors are presented in Fig. 4. The errors with the ESIE+SS method might be dominated by the 3D-representation of a 2D case, with a mix of approaches for the various components of the  $G$  and  $H$  transfer functions. For the higher frequencies, the number of secondary sources might contribute to the discrepancy. The results can be viewed as accurate, with 5%- and 95%-percentile values for the error of the whole set of  $181 \cdot 21 = 3801$  data points being, respectively, -0.30 dB and +0.33 dB, with a median error of -0.04 dB.

The computation load for the ESIE+SS method is much higher than for the FEM since the study of a 2D case actually requires more computations than a 3D case, with the ESIE(+SS) method. The efficiency of the ESIE+SS method for 3D cases will be studied in future work.

#### 5. CONCLUSIONS

It has been demonstrated that secondary sources in a rigid scattering object can simulate impedance boundary conditions for parts of the scattering object. For the presented numerical comparisons, a 3D version of a 2D case was implemented using the ESIE diffraction method, and 2D

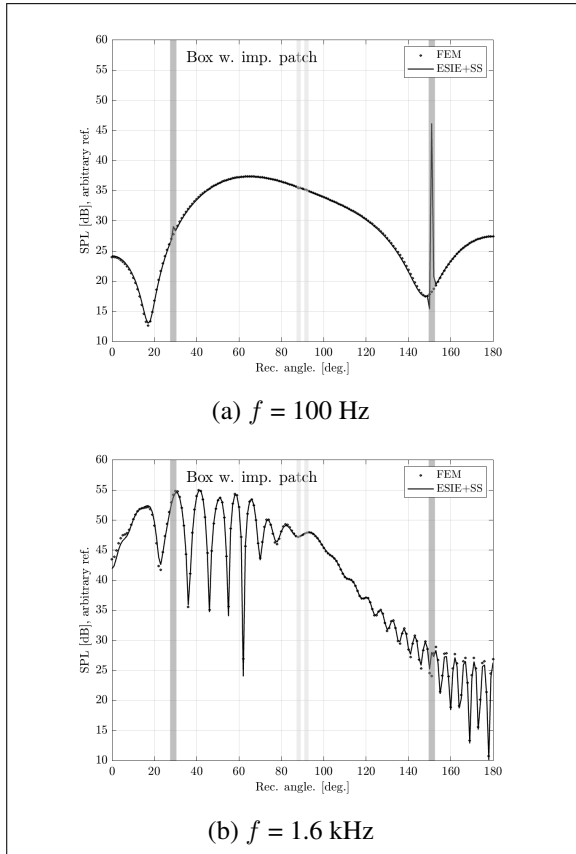


**Figure 3:** Computed results for two frequencies. Grey areas indicate receivers with known numerical challenges for the ESIE method.

$f$ [Hz]	Length $L$ [m]	$N_{SS}$	Gaussian quad.
50-125	40	2	449
160-400	20	2	399
500-1k	10	5	399
1.25k-2.5k	7	11	449

**Table 1:** Numerical settings for the secondary source method, "ESIE+SS"

FEM calculations were used as reference. The agreement was excellent except for a few known problem receiver positions. The method seems to have good potential for 3D scattering cases where the scattering object has small impedance parts in a largely rigid object.

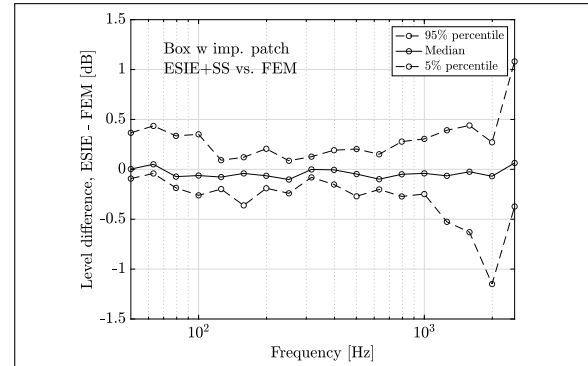


**Figure 4:** Median values, with 95% and 5% percentiles, across the 181 receiver positions.

## 6. ACKNOWLEDGMENTS

This research was funded by the Norwegian Defence Estates Agency.

## 7. REFERENCES

- [1] A. Asheim and U. P. Svensson, "An integral equation formulation for the diffraction from convex plates and polyhedra," *J. Acoust. Soc. Am.*, vol. 133, pp. 3681–3691, 2013.
- [2] S. R. Martin, U. P. Svensson, J. Slechta, and J. O. Smith, "Modeling sound scattering using a combination of the edge source integral equation and the boundary element method," *J. Acoust. Soc. Am.*, vol. 144, pp. 131–141, 2018.
- [3] G. Pavic and L. Du, "Modelling of multi-connected acoustical spaces by the surface impedance approach," in *Internoise Hamburg 2016*, pp. 4278–4287, 2016.
- [4] "COMSOL." [www.comsol.com](http://www.comsol.com), 2022.
- [5] "Norflag." [web2.norsonic.com](http://web2.norsonic.com), 2022.
- [6] U. P. Svensson, "Edge diffraction Matlab toolbox." [https://github.com/upsvensson/Edge-diffraction\\_Matlab\\_toolbox](https://github.com/upsvensson/Edge-diffraction_Matlab_toolbox), 2022.
- [7] I. Tolstoy, "Exact, explicit solutions for diffraction by hard sound barriers and seamounts," *J. Acoust. Soc. Am.*, vol. 85, pp. 661–669, 1989.
- [8] U. P. Svensson, K. Sakagami, and M. Morimoto, "Line integral model of transient radiation from planar pistons in baffles," *Acta Acust. Acust.*, vol. 87, pp. 307–315, 2001.